

Metamaterial transparency induced by cooperative electromagnetic interactions

Stewart D. Jenkins and Janne Ruostekoski

*School of Mathematics and Centre for Photonic Metamaterials,
University of Southampton, Southampton SO17 1BJ, United Kingdom*

(Dated: October 9, 2018)

We propose a cooperative asymmetry-induced transparency, CAIT, formed by collective excitations in metamaterial arrays of discrete resonators. CAIT can display a sharp transmission resonance even when the constituent resonators individually exhibit broad resonances. We further show how dynamically reconfiguring the metamaterial allows one to actively control the transparency. While reminiscent of electromagnetically induced transparency, which can be described by independent emitters, CAIT relies on a cooperative response resulting from strong radiative couplings between the resonators.

Electromagnetically induced transparency (EIT), a result of destructive interference between different excitation paths, causes an otherwise opaque collection of electromagnetic (EM) emitters to become transparent over a range of frequencies. In atomic gases, interference between atomic level transitions prevents the excitation of a transition that scatters incident light [1–3]. This interference abruptly alters the dispersion relation for frequencies in the transparency window, providing a mechanism to slow [4] or even stop light for later retrieval [5, 6]. Slow and stopped light pulses have led to applications in sensitive magnetometry [7–10], all-optical switching [11], and quantum memories [12–15].

Several theoretical proposals [16–19] and experimental realizations [20–28] have transferred the idea of EIT in independently scattering atoms to metamaterial arrays of circuit elements. In these artificially structured materials, the unit-cell resonators (meta-molecules) play a role analogous to atoms in conventional EIT. A transmission resonance forms via coupling between two modes of plasmonic excitations in independently scattering meta-molecules: a bright mode that strongly radiates and a dark mode with a narrower radiative linewidth. Broad radiative linewidths of nanofabricated circuit elements, however, can severely limit the quality of EIT-like transmission resonances in independently scattering meta-molecules.

Recent studies [29–33] have shown that, rather than independently, certain systems of closely-spaced resonators respond cooperatively to an incident field. In particular, interactions between resonators that are mediated by scattered EM fields result in collective modes of resonator excitations [29], several of which have significantly narrowed radiative linewidths.

In this Letter, we show how to exploit such collective modes to realize a cooperative transmission resonance. We propose a cooperative asymmetry-induced transparency (CAIT) in metamaterials. Unlike transmission resonances based on independent scatterers, the bright and dark modes in CAIT are collective. Specifically, the dark mode possesses a cooperatively narrowed resonance linewidth. This narrowing leads to a sharp resonance of high transmission, even though the resonators forming the metamaterial would individually, in isola-

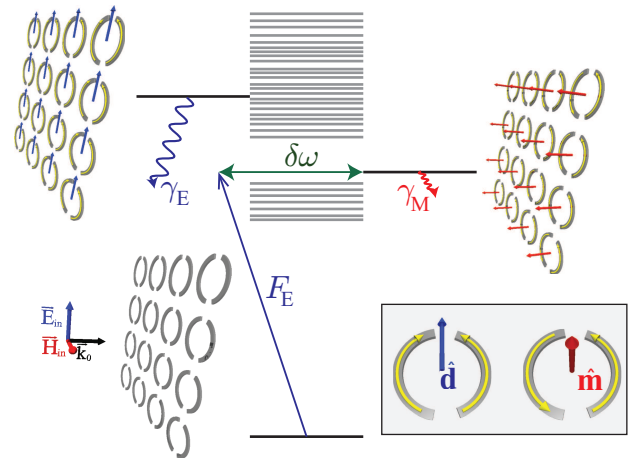


FIG. 1. (Color online) A schematic illustration of CAIT in an array of ASRs. The inset shows symmetric (antisymmetric) currents in the ASR meta-atoms producing electric (magnetic) dipoles along $\hat{\mathbf{d}}$ ($\hat{\mathbf{m}}$). The PME (PMM) mode is illustrated in the upper left (upper right), and has a decay rate γ_E (γ_M). An incident wave couples an unexcited (lower) array to the PME mode with strength F_E , while asymmetry $\delta\omega$ induces a coupling between the PME and PMM modes. The grey lines represent other collective modes.

tion, exhibit broad resonances.

The transmission resonance is sensitive to the size of the system and the specific resonator configuration. Limited only by intrinsic nonradiative losses, the transmission resonance and group delay of a transmitted pulse can become progressively narrower and longer, respectively, with increasing size of a two-dimensional (2D) metamaterial array. In a 205×205 array, for example, we estimate the resonance width (pulse delay) to be approximately $\Gamma/1000$ ($1600/\Gamma$), where Γ is the linewidth of a single isolated resonator. Furthermore, changing relative positions of the resonators alters the EM mediated interactions between them, and hence the cooperative material response. We show that using reconfigurable metamaterials [34, 35], in which one can dynamically shift the layout of the metamolecules, allows one to actively control the transparency.

To illustrate CAIT, we consider a 2D array of asym-

metric split rings (ASRs) [31, 36], consisting of pairs of concentric circular arcs (Fig. 1). The setup is closely related to recent transmission resonance experiments [31]. In each ASR, currents can flow symmetrically, producing a net electric dipole along the direction $\hat{\mathbf{d}}$, or antisymmetrically, producing a net magnetic dipole along $\hat{\mathbf{m}}$. CAIT forms from the coupling between two phase-coherent collective modes of ASR excitations that are phase-matched with an incident EM plane wave propagating perpendicular to the array. The incident field drives the phase-matched electric (PME) mode, dominated by all electric dipoles oscillating in phase, while the phase-matched magnetic (PMM) mode, consisting almost entirely of magnetic dipoles perpendicular to the array, does not directly couple to the incident field. In an array with subwavelength lattice spacing, the radiative linewidth of the PMM mode γ_M narrows with the system size. Because it radiates only weakly [30], the PMM mode can be used as a collective dark-mode in CAIT. For example, in a 33×33 array of split rings separated by half a wavelength, cooperative interactions reduce γ_M fifty fold [29]. An excited PME mode, on the other hand, radiates with rate $\gamma_E \gg \gamma_M$, scattering the field into the forward and backward directions and reflecting the incident field. We will show how a transmission resonance with an active control forms via an interference that permits excitation of the cooperatively narrowed PMM mode at the expense of the PME mode.

We consider a 2D square lattice of identical ASRs in the $z = 0$ plane with subwavelength lattice-spacing a and lattice vectors $\mathbf{a}_1 = a\hat{\mathbf{e}}_x$ and $\mathbf{a}_2 = a\hat{\mathbf{e}}_y$. The ASR electric (magnetic) dipoles – produced by symmetric (antisymmetric) current oscillations – are oriented along $\hat{\mathbf{d}} = \hat{\mathbf{e}}_y$ ($\hat{\mathbf{m}} = \hat{\mathbf{e}}_z$); Fig. 1. Each ASR, labeled by index ℓ ($\ell = 1 \dots N$), comprises two meta-atoms (circular arcs). A meta-atom, labeled by index j ($j = 1 \dots 2N$), behaves as a radiatively damped LC circuit which is driven by the incident field and the fields emitted by all other meta-atoms in the system [29]. We describe the current flow in meta-atom j by a slowly varying complex amplitude b_j . (See Appendix A for technical details.) The meta-atom resonance frequencies are centered on ω_0 . Owing to an asymmetry in arc lengths, the resonance frequencies of the right ($j = 2\ell$) and left ($j = 2\ell - 1$) meta-atoms in each ASR are shifted by $\delta\omega$ and $-\delta\omega$, respectively. The oscillating electric and magnetic dipoles of each meta-atom radiate at respective rates Γ_E and Γ_M .

To better understand how a collection of ASRs behaves in concert, we first examine a single, isolated ASR of two interacting arcs. The dynamics of an ASR ℓ can be described by the amplitudes of symmetric, $c_{\ell,+}$, and antisymmetric, $c_{\ell,-}$, current oscillations, which are given in terms of the meta-atom variables as $c_{\ell,\pm} = (b_{2\ell} \pm b_{2\ell-1})/\sqrt{2}$. These oscillations are eigenmodes of a single symmetric split ring (SSR) ($\delta\omega = 0$) with the radiative decay rates $\gamma_+ \approx 2\Gamma_E$ and $\gamma_- \approx 2\Gamma_M$ and resonance frequencies $\omega_0 \pm \delta$.

In a single ASR the asymmetry shifts the resonance

frequencies of the left and right arcs. As a result, the symmetric and antisymmetric oscillations are no longer eigenmodes of a single ASR, and the evolution of those oscillations becomes coupled

$$\dot{c}_{\ell,\pm} = (-\gamma_{\pm}/2 \mp i\delta) c_{\ell,\pm} - i\delta\omega c_{\ell,\mp} + F_{\ell,\pm}, \quad (1)$$

where $F_{\ell,\pm}$ represents the external driving. An EIT-like resonance of independently scattering ASRs requires that $\gamma_{\mp} \ll \gamma_{\pm}$. This would allow the dark mode (with lower emission rate) to be highly excited so that the coupling $\delta\omega$ to the bright mode (with higher emission rate) destructively interferes with driving of the bright mode by the incident field. In most experimental situations involving ASRs [31, 36], however, γ_+ and γ_- are comparable. An array of independently scattering ASRs therefore cannot exhibit an EIT-like transmission resonance.

The situation differs, however, in a metamaterial array of several ASRs that interact via scattered EM fields. As a result of interactions, the system possesses collective modes of oscillation extended over the metamaterial. To show how CAIT can emerge from these collective modes, we construct an approximate phenomenological model from the PME and PMM modes, the two collective modes that are phase matched with the incident field. We use this model to analytically calculate the steady-state reflectance and transmittance. The mode properties, the accuracy of the phenomenological model, and the role of other collective modes in the metamaterial's EM response are numerically determined using the formalism introduced in Ref. [29]. These calculations fully incorporate all dependent scattering processes [29, 37–42] between the resonators to all orders. Applying the formalism to a 2D array of ASRs [30] yielded a narrowing of collective linewidths with system size that agreed extremely well with experimental measurements of transmission resonances [31].

In the analysis, we approximate the incident EM field by a monochromatic plane wave and write the positive frequency component of the electric field amplitude $\mathbf{E}_{\text{in}}^+(\mathbf{r}, t) = \mathcal{E} \hat{\mathbf{e}}_y e^{i\mathbf{k}_{\text{in}} \cdot \mathbf{r} - i\Omega t}$, where $\hat{\mathbf{e}}_y$ and $\mathbf{k}_{\text{in}} = k\hat{\mathbf{e}}_z$ ($k = \Omega/c$) denote the polarization and wavevector, respectively. The collective dynamics of the full metamaterial system, described by meta-atom variables $\mathbf{b} \equiv (b_1, b_2, \dots, b_{2N-1}, b_{2N})^T$, is governed by [29, 30]

$$\dot{\mathbf{b}} = \mathcal{C}\mathbf{b} + \mathbf{F}(t), \quad \mathcal{C} = \mathcal{C}_{\text{SSR}} - i\delta\omega\mathcal{A}. \quad (2)$$

In the radiative dynamics of the meta-atoms, described by \mathcal{C} , we separate the contributions of \mathcal{C}_{SSR} and $i\delta\omega\mathcal{A}$, so that the matrix \mathcal{C}_{SSR} describes the collective dynamics of the metamaterial in the absence of asymmetry (i.e. in an array where all ASRs are replaced by SSRs), and $\delta\omega\mathcal{A}$ accounts for the resonance shifts of the individual meta-atoms due to the asymmetry of the ASRs. The diagonal elements of the interaction matrix $\mathcal{C}_{\text{SSR},j,j} = -\Gamma/2$, where $\Gamma \equiv \Gamma_E + \Gamma_M$, represent decay rates and its off-diagonal elements interactions mediated by the scattered EM field. The asymmetry in the ASRs shifts the meta-

atom resonance frequencies by $\pm\delta\omega$. The sign of the frequency shift for a given meta-atom is contained in the diagonal matrix $\mathcal{A} = \text{diag}(-1, 1, \dots, -1, 1)$; the alternating signs of the elements indicate that the asymmetry shifts the frequencies of each side of the ASR in opposite directions. As a result of the incident wave, each element j also experiences a driving $F_j = F_0 \exp[i(\mathbf{k} \cdot \mathbf{r} - \Delta t)]$, $\Delta \equiv \Omega - \omega_0$, with uniform amplitude F_0 .

In the following analysis, it is beneficial to consider the collective modes that are eigenvectors of \mathcal{C}_{SSR} , i.e., eigenmodes of a metamaterial in the absence of meta-molecule asymmetries. Of particular interest among the collective modes are the PME and PMM modes with phase-coherent electric and magnetic dipole excitations, respectively. The incident wave, whose electric field is parallel to the ASR electric dipoles, drives the PME mode. Since the incident wave's magnetic field is perpendicular to the ASR magnetic dipoles, the PMM mode is not directly driven. The asymmetry, however, couples the collective modes to each other in a way similar to how it couples the symmetric and antisymmetric oscillations of a single isolated ASR (See Appendix B). The phases and amplitudes of the electric dipoles in the PME mode closely match those of the magnetic dipoles in the PMM mode. Because of this mode matching, the asymmetry couples the PME and PMM modes more strongly to each other than to any other mode in the system. We therefore initially ignore coupling of other collective modes to the PME and PMM modes. (This is later justified by the full numerical calculation and in Appendix B.) The dynamics is therefore approximated by,

$$\dot{c}_{\text{E}} = (-i\delta_{\text{E}} - \gamma_{\text{E}}/2) c_{\text{E}} - i\delta\omega c_{\text{M}} + f_{\text{E}} \quad (3a)$$

$$\dot{c}_{\text{M}} = (-i\delta_{\text{M}} - \gamma_{\text{M}}/2) c_{\text{M}} - i\delta\omega c_{\text{E}}, \quad (3b)$$

where the subscripts E and M refer to PME and PMM modes, respectively (excitation amplitudes $c_{\text{E,M}}$, resonance frequency shifts $\delta_{\text{E,M}}$, decay rates $\gamma_{\text{E,M}}$, and driving f_{E}). Equations (3a) and (3b) are similar to those that describe the dynamics of atomic coherences in EIT [3]. Namely, when the system is driven on resonance with the PMM mode and $(\delta\omega)^2 \gg \gamma_{\text{M}}\gamma_{\text{E}}$, the PMM mode is excited and the asymmetry induced coupling between the PMM and PME destructively interferes with the driving of the PME mode to prevent its excitation.

In the calculation of the transmittance and reflectance we consider the field scattered from the resonators in the forward, $\hat{\mathbf{e}}_z$, and backward, $-\hat{\mathbf{e}}_z$, directions in the far field. We assume an absorbing planar barrier is placed around the metamaterial array so that the incident field can propagate through the array, but not around it, yielding the diffracted far field component of the incident field in the forward direction, $E_{\text{I}} \equiv \hat{\mathbf{d}} \cdot \mathbf{E}_{\text{I}}(\hat{\mathbf{e}}_z)$ (See Appendix C). Both the incident and the scattered fields $\mathbf{E}_{\text{S}}(\pm\hat{\mathbf{e}}_z)$ are polarized along the meta-atom electric dipoles. Therefore, we define the transmittance and reflectance amplitudes as $T = (E_{\text{I}} + \hat{\mathbf{d}} \cdot \mathbf{E}_{\text{S}}(\hat{\mathbf{e}}_z))/E_{\text{I}}$ and $R = \hat{\mathbf{d}} \cdot \mathbf{E}_{\text{S}}(-\hat{\mathbf{e}}_z)/E_{\text{I}}$ (See Appendix C).

Array Size	$\delta\omega/\Gamma$	δ_{E}/Γ	γ_{E}/Γ	δ_{M}/Γ	γ_{M}/Γ
small: 11×11	0.1	0.76	1.5	0.57	0.034
medium: 41×41	0.1	0.79	1.5	0.56	3.0×10^{-3}
large: 205×205	0.02	0.79	1.5	0.56	1.2×10^{-4}

TABLE I. The ASR asymmetries and the PME and PMM mode properties of the 2D ASR arrays used to demonstrate CAIT. The linewidth γ_{M} varies inversely with the size of the array.

We first estimate R and T in a phenomenological model by solving the steady-state response of Eqs (3) and assuming a uniformly excited array. This simplified approach is then compared with a full numerical solution of Eq. (2) that incorporates all collective modes and the finite-size effects. In the phenomenological uniform mode approximation (See Appendix E), we find

$$R = \frac{R_0 \gamma_{\text{E}}/2 [\gamma_{\text{M}}/2 - i(\Delta - \delta_{\text{M}})]}{(\delta\omega)^2 - (\Delta - \delta_{\text{E}} + i\gamma_{\text{E}}/2)(\Delta - \delta_{\text{M}} + i\gamma_{\text{M}}/2)}, \quad (4)$$

and $T = 1 + R$, where $R_0 = -3(\Gamma_{\text{E}}/\gamma_{\text{E}})/[2\pi(a/\lambda)^2]$ is the reflectance of the system on resonance with the PME mode when $\delta\omega = 0$, and $\lambda \equiv c/(2\pi\omega_0)$. The phenomenological model (4) depends on the parameters of the collective modes PME and PMM, $\gamma_{\text{E,M}}$ and $\delta_{\text{E,M}}$, that may be calculated numerically (See Appendix E3). Some example values are given in Table I. To illustrate the cooperative nature of CAIT, we here examine the transmission properties of three different sized arrays: a small (11×11), medium (41×41), and large (205×205). All have lattice spacing $a = 0.4\lambda$, $\Gamma_{\text{E}} = \Gamma_{\text{M}}$, and are composed of ASRs whose meta-atoms are separated by $u = 0.18\lambda$.

Figure 2 shows that, in the medium array, the uniform mode approximation reproduces the qualitative behavior of the full model [Eq. (2)]. This correspondence indicates that the PME and PMM modes play the dominant role in governing the array's transmission properties. The discrepancy arises due to finite-size effects in the full model, which, for example, allow the excitation of modes other than the PME and PMM modes.

Comparing the transmission spectra in Fig. 2, one finds that the medium and large arrays support CAIT, while the small array does not. When $\gamma_{\text{M}} \ll (\delta\omega)^2/\gamma_{\text{E}}$, as in the medium and large arrays, excitation of the PME mode is suppressed in a range of frequencies around the PMM resonance (See Appendix E). This suppression reduces reflection, opening a transparency window. Equation (4) indicates that resonant driving of the PMM maximizes the intensity transmittance when $|\delta_{\text{E}} - \delta_{\text{M}}| \ll \gamma_{\text{E}}$. The quality, or inverse spectral width, of the resonance increases in proportion to $(\delta\omega)^{-2}$ (See Appendix F). But the condition $\gamma_{\text{M}} \ll (\delta\omega)^2/\gamma_{\text{E}}$ imposes an upper bound on the achievable quality, as illustrated by the lack of a transparency window for the small array.

In contrast to EIT, the decay rate of the cooperative dark mode asymptotically scales as $\gamma_{\text{M}} \sim 1/N$ with the

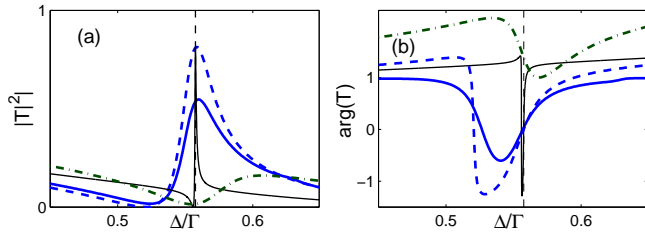


FIG. 2. (Color online) (a) The intensity transmittance $|T|^2$ and (b) the phase delay $\arg(T)$ of the small ASR array in the full model (dot-dashed green line), the medium array in the full model (solid blue line), the medium array in the uniform mode approximation (dashed blue line), and the large array in the uniform mode approximation (thin black line). Simultaneously increasing the array size and reducing the asymmetry narrows the CAIT resonance.

number N of ASRs [30]. This permits one to narrow the transparency window by designing an array with a greater N and reduced $\delta\omega$, even when the constituent resonators individually would exhibit broad linewidths. On PMM resonance, Eq. (4) implies that the minimum asymmetry required to suppress R below a given level $\delta\omega_{\min} \propto \sqrt{\gamma_M}$ (See Appendix F). Hence the maximum attainable quality factor [$\propto (\delta\omega)^{-2}$] of the transparency window increases in proportion to N and is eventually only limited by nonradiative losses, resulting in very sharp resonances with high modulation depths. For example, from the asymptotic expressions of $\gamma_{E,M}$ and $\delta_{E,M}$ (See Appendix E3) we can deduce that simultaneously quintupling the side lengths of an array and reducing $\delta\omega$ by a factor of five narrows the resonance from about $\Gamma/40$ to $\Gamma/1000$ (Appendix D), while maintaining the peak transmittance (Fig. 2).

The sharp transmission resonance exhibits a considerable phase delay $\varphi(\Delta) \equiv \arg(T(\Delta))$ on Δ . According to numerics a pulse resonant on the PMM mode passing through the 41×41 sample would experience a group delay of $\tau_g \equiv d\varphi/d\Delta|_{\Delta=\delta_M} \approx 47/\Gamma$. The delay is further enhanced in the large array owing to linewidth narrowing and we estimate $\tau_g \approx 1600/\Gamma$ in the phenomenological model.

Dynamically reconfiguring the metamaterial geometry [34, 35] provides an active control mechanism for the transparency. To illustrate this, we split the medium array into two interleaved sublattices with lattice vectors $\mathbf{a}_1 = 2a\hat{\mathbf{e}}_x$ and $\mathbf{a}_2 = a\hat{\mathbf{e}}_y$. The lattices are displaced from one and other by $a\hat{\mathbf{e}}_x + \delta\mathbf{R}$ so that for $\delta\mathbf{R} = 0$, the ASRs form a square lattice. Figure 3 shows how distorting the lattice alters the transmission resonance. Displacing the sublattices by $\delta\mathbf{R} = -0.1\lambda\hat{\mathbf{e}}_z$ generates a relative shift of about 0.5Γ between the PME and PMM resonances, almost entirely eliminating the transparency. A fast control of metamaterial arrays [35], together with the sensitivity of cooperative resonances to the specific resonator configuration, could potentially open possibilities for stopped pulse and light storage applications [5].

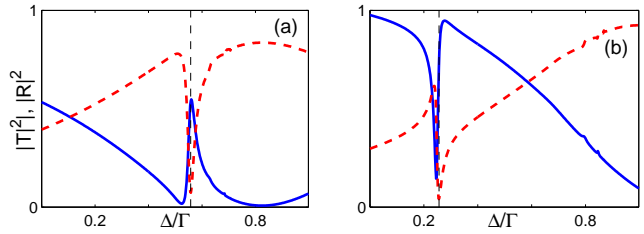


FIG. 3. (Color online) The effect of reconfiguring the metamaterial geometry on the transmission resonance. The intensity transmittance (solid line) and intensity reflectance (dashed line) are calculated for a (a) 41×41 2D array and (b) a lattice in which the two sublattices are shifted by $\delta\mathbf{R} = 0.1\lambda\hat{\mathbf{e}}_z$. Calculations account for excitation of and scattering from all collective modes. The vertical dashed lines indicate the PMM resonance.

In conclusion, we proposed a controllable mechanism to produce a cooperative transmission resonance CAIT. Whereas standard EIT can be described by independent emitters, CAIT relies on a cooperative response of the metamaterial. A transmission resonance forms when a subradiant collective mode, acting as a dark state, is excited at the expense of the mode that most efficiently couples to an incident EM field. Since the lifetime of the dark PMM mode increases with size of the array [30], the attainable quality of the resonance scales in proportion with the number of resonators in the metamaterial. For large arrays, only nonradiative decay, which could be incorporated into the analysis using a phenomenological parameter [30], limits the attainable quality factor of the resonance. In low-loss materials, such as superconducting metamaterial arrays [43–48], the nonradiative decay, however, can be suppressed.

ACKNOWLEDGMENTS

This work was supported by the EPSRC and the Leverhulme Trust. We would like to thank N. Papasimakis, V. Fedotov, V. Savinov, E. Plum, M. D. Lee, M. O. Borgh and N. I. Zheludev for discussions.

Appendix A: Asymmetric split rings in the metamaterial array

We base our analysis of the CAIT response on a general formalism we developed [29] to describe collectively interacting metamaterial arrays of magnetodielectric resonators. When applied to 2D arrays of strongly coupled asymmetric split rings (ASRs), this model yielded an excellent agreement [30] with the experimental transmission resonance measurements in Ref. [29].

To show how CAIT arises from cooperative phenomena, we consider an ensemble of N identical ASRs, each composed of two circular arcs, or meta-atoms (see Fig. 1),

lying on or near (within a tenth of a wavelength) of the $z = 0$ plane. The meta-atoms are labeled by indices j ($j = 1, \dots, 2N$) such that ASR ℓ ($\ell = 1, \dots, N$) comprises meta-atoms $2\ell - 1$ and 2ℓ . Although, in general, each meta-atom j occupies an area comparable to that of the metamaterial unit-cell [31], we can produce the qualitative behavior of an ASR by approximating meta-atom j as a point source for the electromagnetic (EM) field at position \mathbf{r}_j , where the arcs of an ASR are separated by $\mathbf{u} \equiv \mathbf{r}_{2\ell} - \mathbf{r}_{2\ell-1} \equiv u\hat{\mathbf{u}}$ [30]. In this work, we assume the ASRs are oriented such that $\hat{\mathbf{u}} = \hat{\mathbf{e}}_x$.

We assume each meta-atom j supports a single mode of current oscillation that behaves as an effective LC circuit with resonance frequency ω_j [29]. If the split rings were symmetric, the individual meta-atoms would have identical resonance frequencies $\omega_j = \omega_0$. An asymmetry in the arc lengths shifts the meta-atom resonance frequencies by $\delta\omega$ so that for ASR ℓ

$$\omega_{2\ell-1} = \omega_0 - \delta\omega, \quad (\text{A1a})$$

$$\omega_{2\ell} = \omega_0 + \delta\omega. \quad (\text{A1b})$$

Oscillating currents in meta-atom j produce an electric dipole $\mathbf{d}_j(t) = d_j(t)\hat{\mathbf{d}}$ and magnetic dipole $\mathbf{m}_j(t) = m_j(t)\hat{\mathbf{m}}_j$, where d_j and m_j are the electric and magnetic dipole amplitudes, respectively. The resulting electric and magnetic dipole radiation damps current oscillations in the meta-atom at rates Γ_E and Γ_M , respectively [29]. All ASRs in the array have the same orientation so that every meta-atom's electric dipole points in the direction $\hat{\mathbf{d}} \equiv \hat{\mathbf{e}}_y$. The magnetic dipole directions $\hat{\mathbf{m}}_j$, on the other hand, are oriented so that identical current flows in an ASR produce opposite magnetic dipoles in its constituent meta-atoms. That is, the right ($j = 2\ell$) and left ($j = 2\ell - 1$) meta-atoms in ASR ℓ have magnetic dipole orientations $\hat{\mathbf{m}}_{2\ell} = -\hat{\mathbf{m}}_{2\ell-1} \equiv \hat{\mathbf{m}} = \hat{\mathbf{u}} \times \hat{\mathbf{d}} = \hat{\mathbf{e}}_z$. In this way, identical current flows in an ASR's meta-atoms produce an electric dipole, while equal and opposite flows produce a magnetic dipole. The dynamics of the oscillating dipoles within each meta-atom j are described by the slowly varying normal variable [29]

$$b_j(t) = \sqrt{\frac{k_0^3}{12\pi\epsilon_0}} \left(\frac{d_j(t)}{\sqrt{\Gamma_E}} + i \frac{m_j(t)}{c\sqrt{\Gamma_M}} \right), \quad (\text{A2})$$

where $k_0 \equiv \omega_0/c$.

Appendix B: Asymmetry induced coupling of collective modes

In this appendix, we show how the asymmetry in the ASRs couples collective modes of the system. Of particular importance to CAIT are the phase matched electric (PME) mode, in which all electric dipoles oscillate in phase, and the phase matched magnetic (PMM) mode, in which all magnetic dipoles oscillate in phase. The PME mode is phase-matched with EM plane-waves propagating perpendicular to the array and can be easily excited

by an incident field. For ASRs in a square lattice, we show that the PME and PMM modes couple almost exclusively to each other. This exclusivity yields the simplified response of the PME and PMM modes described by Eqs. (3).

To describe the dynamics of the metamaterial comprising an ensemble of ASRs, we employ the column vector of normal variables,

$$\mathbf{b}(t) = \begin{pmatrix} b_1(t) \\ b_2(t) \\ \vdots \\ b_{2N-1}(t) \\ b_{2N}(t) \end{pmatrix}. \quad (\text{B1})$$

We associate collective modes of the system with eigenvectors of \mathcal{C}_{SSR} , i.e., eigenmodes of a metamaterial where all ASRs are replaced by symmetric split rings (SSRs). The n^{th} collective mode corresponds to the eigenvector \mathbf{v}_n of the interaction matrix \mathcal{C}_{SSR} normalized such that $\mathbf{v}_m^T \mathbf{v}_n = \delta_{mn}$. The state $\mathbf{b}(t)$ can be expanded as

$$\mathbf{b}(t) = \sum_n c_n(t) \mathbf{v}_n, \quad (\text{B2})$$

where $c_n(t) \equiv \mathbf{v}_n^T \mathbf{b}(t)$ is the amplitude of the collective mode n . By expressing \mathbf{b} in the basis of collective modes $\{\mathbf{v}_n : n = 1, \dots, 2N\}$, we find that the asymmetry results in the evolution of the amplitudes,

$$\dot{c}_n = (-i\delta_n - \gamma_n/2) c_n - i\delta\omega \sum_m c_m (\mathbf{v}_n^T \mathcal{A} \mathbf{v}_m) + f_n, \quad (\text{B3})$$

where δ_n and γ_n are the frequency shift and decay rate of mode n , corresponding to the n^{th} eigenvalue of \mathcal{C}_{SSR} . The matrix element $(\mathbf{v}_n^T \mathcal{A} \mathbf{v}_m)$ represents the coupling between modes m and n , caused by the asymmetry.

We identify the PME (PMM) mode as the eigenvector of \mathcal{C}_{SSR} that most resemble all electric (magnetic) dipoles oscillating in phase with equal amplitudes [30]. The coupling between the PME amplitude c_E and the PMM amplitude c_M , given by $\mathbf{v}_M^T \mathcal{A} \mathbf{v}_E$, can dominate over their coupling to other modes for particular arrangements of ASRs. For example, in the 41×41 (medium) array considered in the main text, the asymmetric coupling coefficient is $|\mathbf{v}_M^T \mathcal{A} \mathbf{v}_E| \approx 0.9993$ and the maximal coupling of the PME and PMM modes to other collective modes is $\mathbf{v}_n^T \mathcal{A} \mathbf{v}_E, \mathbf{v}_n^T \mathcal{A} \mathbf{v}_M < 0.04$ for $n \notin \{E, M\}$. The PME and PMM modes thus obey the simplified dynamics given by Eqs. (3).

In sum, if the incident field does not directly drive any other modes, the near exclusive coupling of the PME and PMM modes to each other forms an effective two-mode system for the metamaterial. This further justifies the use of the phenomenological model in the main text.

Appendix C: Scattered light, transmittance and reflectance

To analyze the light scattering properties of the array, including its reflectance and transmittance, we consider a plane wave of frequency Ω impinging on the array with positive frequency component

$$\mathbf{E}_{\text{in}}^+(\mathbf{r}, t) = \hat{\mathbf{d}}\mathcal{E}e^{i(kz - \Omega t)}, \quad (\text{C1})$$

where $k \equiv \Omega/c$, and \mathcal{E} is the electric field amplitude. The incident wave is detuned from the central meta-atom resonance frequency by $\Delta \equiv \Omega - \omega_0$. According to Eq. (2), driving by the incident wave induces a cooperative response of the array. The oscillating electric and magnetic dipoles emit a scattered field \mathbf{E}_{S} .

So as to consider the transmittance through the meta-material array, we assume a 2D barrier is placed around the array in the $z = 0$ plane so that fields can propagate through the array, but not around it. We denote the incident field that would diffract through the barrier if the array were not present as \mathbf{E}_{I} . The field transmitted through the array ($z > 0$) is then $\mathbf{E}_{\text{T}} \equiv \mathbf{E}_{\text{I}} + \mathbf{E}_{\text{S}}$. On the other hand, the field reflected from the array ($z < 0$) is determined only by the scattered field \mathbf{E}_{S} .

For simplicity, we analyze the diffracted and scattered fields in the far field, observed a distance R from the metamaterial much greater than the spatial extent of the array. Here, we define the far field amplitude $\mathbf{E}(\hat{\mathbf{k}}, \Omega)$ of the electric field along the direction $\hat{\mathbf{k}}$ (with wavevector $\mathbf{k} = k\hat{\mathbf{k}}$) such that the positive component of the electric field at $R\hat{\mathbf{k}}$,

$$\mathbf{E}^+(R\hat{\mathbf{k}}, t) \approx \frac{e^{i(kR - \Omega t)}}{kR} \mathbf{E}(\hat{\mathbf{k}}, \Omega). \quad (\text{C2})$$

According to Fraunhofer diffraction [49], the diffracted incident field then reads

$$\mathbf{E}_{\text{I}}(\hat{\mathbf{k}}) = -ik^2 (\hat{\mathbf{k}} \times \hat{\mathbf{e}}_x) \frac{1}{2\pi} \int_A dx dy \mathcal{E} e^{-i\mathbf{k} \cdot \mathbf{r}_{\perp}}, \quad (\text{C3})$$

where A is the area of the aperture, and $\mathbf{r}_{\perp} \equiv x\hat{\mathbf{e}}_x + y\hat{\mathbf{e}}_y$. The barrier that surrounds an $N_x \times N_y$ lattice centered at the origin contains an $N_x a \times N_y a$ rectangular aperture where a is the lattice spacing. From Eq. (C3), the forward diffracted component of the incident field through such a barrier is therefore given by

$$\mathbf{E}_{\text{I}}(\hat{\mathbf{k}}) = -i \frac{N\mathcal{E}(ka)^2}{2\pi} (\hat{\mathbf{k}} \times \hat{\mathbf{e}}_x) \prod_{j=x,y} \text{sinc}\left(\frac{N_j k_j a}{2}\right), \quad (\text{C4})$$

The scattered fields, on the other hand, result from electric and magnetic dipole radiation emitted by the meta-atoms. Their far-field components are given by [49]

$$\mathbf{E}_{\text{S}}(\hat{\mathbf{k}}, \Omega) = \frac{k^3}{4\pi\epsilon_0} \hat{\mathbf{k}} \times \sum_{j=1}^{2N} \left[(\tilde{\mathbf{d}}_j \times \hat{\mathbf{k}}) - \frac{\tilde{\mathbf{m}}_j}{c} \right] e^{-i\mathbf{k} \cdot \mathbf{r}_j}, \quad (\text{C5})$$

where $\tilde{\mathbf{d}}_j \equiv e^{i\Omega t} \mathbf{d}_j^+$ and $\tilde{\mathbf{m}}_j \equiv e^{i\Omega t} \mathbf{m}_j^+$ are the slowly varying electric and magnetic dipoles, respectively, of meta-atom j . From Eq. (A2), which relates the electric and magnetic dipoles to the amplitudes b_j , we can express the scattered far field amplitude as

$$\mathbf{E}_{\text{S}}(\hat{\mathbf{k}}, \Omega) = -\sqrt{\frac{3k^3}{16\pi\epsilon_0}} \hat{\mathbf{k}} \times \sum_{j=1}^{2N} \left[\sqrt{\Gamma_{\text{E}}} (\hat{\mathbf{k}} \times \hat{\mathbf{d}}) + i(-1)^j \sqrt{\Gamma_{\text{M}}} \hat{\mathbf{m}} \right] b_j(\Delta) e^{-i\mathbf{k} \cdot \mathbf{r}_j}. \quad (\text{C6})$$

In this work, we define the reflectance and transmittance in terms of the backward ($\hat{\mathbf{k}} = -\hat{\mathbf{e}}_z$) and forward scattered ($\hat{\mathbf{k}} = \hat{\mathbf{e}}_z$) fields, respectively. Since the electric dipoles and incident field are oriented along $\hat{\mathbf{d}} = \hat{\mathbf{e}}_y$, and the magnetic dipoles are parallel to $\hat{\mathbf{e}}_z$, the forward and backward scattered fields will be polarized along $\hat{\mathbf{d}}$. We therefore define the forward transmittance and backward reflectance as

$$R \equiv \frac{\hat{\mathbf{d}} \cdot \mathbf{E}_{\text{S}}(-\hat{\mathbf{e}}_z, \Omega)}{\hat{\mathbf{d}} \cdot \mathbf{E}_{\text{I}}(\hat{\mathbf{e}}_z)}, \quad (\text{C7a})$$

$$T \equiv \frac{\hat{\mathbf{d}} \cdot (\mathbf{E}_{\text{I}}(\hat{\mathbf{e}}_z) + \mathbf{E}_{\text{S}}(\hat{\mathbf{e}}_z, \Omega))}{\hat{\mathbf{d}} \cdot \mathbf{E}_{\text{I}}(\hat{\mathbf{e}}_z)}, \quad (\text{C7b})$$

One could similarly define the reflectance and transmittance amplitudes in terms of the incident and scattered fields integrated over some solid angle about $\pm\hat{\mathbf{e}}_z$. We have checked that in the numerical simulations discussed in the text, integration over a sufficiently small solid angle does not alter the phase or amplitude dependence of the transmitted and reflected fields.

Appendix D: Characterizing a transmission resonance

For a given transmittance amplitude $T(\Delta)$, a transmission resonance occurring at δ_{T} is characterized by peak transmittance $|T(\delta_{\text{T}})|^2$, resonance width w , and group delay τ_g of a resonant pulse passing through the meta-material.

To determine the resonance width, we can approximate the intensity transmittance $|T(\Delta)|^2$ to second order in $\Delta - \delta_{\text{T}}$ by a Gaussian of height $|T(\delta_{\text{T}})|^2$, and full width at half max (FWHM) w . Comparing the Taylor expansions of the two, we have

$$\begin{aligned} |T(\Delta)|^2 &\approx |T(\delta_{\text{T}})|^2 + \frac{1}{2} \frac{d|T|^2}{d\Delta^2} \Big|_{\Delta=\delta_{\text{T}}} (\Delta - \delta_{\text{T}})^2 \\ &\approx |T(\delta_{\text{T}})|^2 \exp\left(-\log 2 \frac{4(\Delta - \delta_{\text{T}})^2}{w^2}\right), \end{aligned} \quad (\text{D1})$$

where the FWHM of the Gaussian is

$$w = \sqrt{-\frac{8(\log 2)|T(\delta_{\text{T}})|^2}{d|T|^2/d\Delta^2 \Big|_{\Delta=\delta_{\text{T}}}}}. \quad (\text{D2})$$

In this work, we estimate the width of the resonance to be the FWHM w of the Gaussian that best fits the intensity transmittance near the peak.

The group delay τ_g of a resonant pulse passing through the metamaterial is determined by the phase of the transmittance amplitude $\arg(T)$. Specifically,

$$\tau_g \equiv \frac{d}{d\Delta} \arg T(\Delta) \Big|_{\Delta=\delta_T} = -i \frac{1}{T} \frac{dT}{d\Delta} \Big|_{\Delta=\delta_T} \quad (\text{D3})$$

Appendix E: The uniform mode approximation for scattering from a planar array

We use the phenomenological two-mode model [Eq. (3)] to estimate the reflectance and transmittance from a uniformly excited planar array of ASRs in which case we neglect boundary effects. We refer to this assumption as the uniform mode approximation. For the uniform PME and PMM modes the frequency shifts $\delta_{E,M}$, collective decay rates $\gamma_{E,M}$, and asymmetry $\delta\omega$ fully describe the cooperative response to an incident plane wave.

We consider an $N_x \times N_y$ ($N = N_x N_y$) square lattice of ASRs with lattice spacing a and lattice vectors $\mathbf{a}_1 = a\hat{\mathbf{e}}_x$ and $\mathbf{a}_2 = a\hat{\mathbf{e}}_y$. In the uniform mode approximation, The PME and PMM modes consist of uniformly excited electric and magnetic dipoles, respectively. Explicitly, these modes correspond to the vectors

$$\mathbf{v}_E = \frac{1}{\sqrt{2N}} \begin{pmatrix} 1 \\ 1 \\ \vdots \\ 1 \\ 1 \end{pmatrix}, \quad \mathbf{v}_M = \frac{1}{\sqrt{2N}} \begin{pmatrix} -1 \\ 1 \\ \vdots \\ -1 \\ 1 \end{pmatrix}. \quad (\text{E1})$$

The alternating signs in \mathbf{v}_M indicate that the currents in each ASR flow out of phase with each other in the PMM mode, while in the PME mode all currents flow in phase. In the uniform mode limit, an incident plane wave propagating perpendicular to the array can only drive the PME mode, while the asymmetry couples the PME and PMM modes only to each other. As such, the metamaterial response to a field of frequency $\Omega = \omega_0 + \Delta$ is given by the Fourier components of the mode amplitudes as

$$\mathbf{b}(\Delta) = c_E(\Delta)\mathbf{v}_E + c_M(\Delta)\mathbf{v}_M. \quad (\text{E2})$$

1. The scattered field in the far field from the steady state metamaterial response

The scattered EM fields are generated by the excitations of the resonators. Each resonator acts as a source of scattered radiation and the regular metamaterial array produces a field pattern of a diffraction grating. In the uniform approximation the excitations are described

by Eq. (E2). The sum over the meta-atoms in the scattered field expression (C6) therefore considerably simplifies. We obtain in the limit $k \approx k_0$

$$E_S(\hat{\mathbf{k}}, \Omega) = -\sqrt{\frac{3Nk^3}{8\pi\epsilon_0}} \mathcal{D}(\mathbf{k}) \hat{\mathbf{k}} \times \left[\left(\hat{\mathbf{k}} \times \hat{\mathbf{d}} \right) \sqrt{\Gamma_E g_E(\hat{\mathbf{k}})} + i\hat{\mathbf{m}} \sqrt{\Gamma_M g_M(\hat{\mathbf{k}})} \right]. \quad (\text{E3})$$

The scattered field is modulated by the diffraction pattern of N unit-cell resonators $\mathcal{D}(\hat{\mathbf{k}}) = \sum_{\ell} e^{-i\mathbf{k} \cdot \mathbf{r}_{\ell}} / N$, where the summation runs over all ASRs ℓ at positions \mathbf{r}_{ℓ} . In the studied system we obtain the familiar field amplitude of a 2D square array of $N_x \times N_y$ diffracting apertures

$$\mathcal{D}(\hat{\mathbf{k}}) = \frac{\sin(N_x k_x a/2) \sin(N_y k_y a/2)}{N \sin(k_x a/2) \sin(k_y a/2)}. \quad (\text{E4})$$

Owing to the subwavelength lattice spacing a , only the zeroth order Bragg peak ($k_x = k_y = 0$) exists. The cone of the emitted radiation in the forward and backward directions $\pm\hat{\mathbf{e}}_z$ narrows as a function of the number of unit-cell resonators N .

In Eq. (E3), $g_E(\hat{\mathbf{k}})$ and $g_M(\hat{\mathbf{k}})$ are, respectively, proportional to the electric and magnetic dipole emission of an ASR along direction $\hat{\mathbf{k}}$. They are given in terms of collective mode amplitudes by

$$g_E(\Delta, \hat{\mathbf{k}}) = c_E \cos\left(\frac{\mathbf{k} \cdot \mathbf{u}}{2}\right) - i c_M \sin\left(\frac{\mathbf{k} \cdot \mathbf{u}}{2}\right), \quad (\text{E5a})$$

$$g_M(\Delta, \hat{\mathbf{k}}) = c_M \cos\left(\frac{\mathbf{k} \cdot \mathbf{u}}{2}\right) - i c_E \sin\left(\frac{\mathbf{k} \cdot \mathbf{u}}{2}\right). \quad (\text{E5b})$$

In the limit $|\mathbf{k} \cdot \mathbf{u}| \ll 1$, the scattered electric (magnetic) dipole radiation is almost solely generated by the PME (PMM) mode. The small mixing of these two contributions results from the finite separation \mathbf{u} of the two meta-atoms in each unit-cell resonator.

We calculate the scattered fields from the steady-state solution of Eqs. (3),

$$c_E = -i \frac{Z_M(\Delta)}{(\delta\omega)^2 - Z_E(\Delta)Z_M(\Delta)} f_E, \quad (\text{E6a})$$

$$c_M = \frac{\delta\omega}{Z_M(\Delta)} c_E, \quad (\text{E6b})$$

where for each mode n , we have defined

$$Z_n(\Delta) \equiv \Delta - \delta_n + i\gamma_n. \quad (\text{E7})$$

The PME and PMM amplitudes are both proportional to the driving $f_E(\Delta)$, which is given by

$$f_E(\Delta) = i \sqrt{\frac{6\pi\epsilon_0}{k^3}} \sqrt{\Gamma_E N} \mathcal{E}. \quad (\text{E8})$$

Having solved the steady-state response of PME mode amplitude [Eq. (E6a)] and the scattered fields emitted

by an excited PME mode [Eq. (E3)], one finds that the incident plane wave produces the forward and backward scattered fields

$$\mathbf{E}_S(\pm\hat{\mathbf{e}}_z, \Omega) = \hat{\mathbf{d}} \frac{3N\Gamma_E}{2} \mathcal{E} \frac{Z_M(\Delta)}{(\delta\omega)^2 - Z_E(\Delta)Z_M(\Delta)}, \quad (\text{E9})$$

2. Reflectance and transmittance

One obtains the transmittance and reflectance by comparing the scattered fields to the forward propagating component of the incident field, $\mathbf{E}_I(\hat{\mathbf{e}}_z)$ [Eq. (C3)]. The reflectance associated with the backward scattered field [Eq. (C7a)] and the transmittance of the forward scattered field [Eq. (C7b)], in the uniform mode approximation, are given by

$$R = \frac{R_0\gamma_E/2 [\gamma_M/2 - i(\Delta - \delta_M)]}{(\delta\omega)^2 - (\Delta - \delta_E + i\gamma_E/2)(\Delta - \delta_M + i\gamma_M/2)}, \quad (\text{E10})$$

$$T = 1 + R, \quad (\text{E11})$$

where

$$R_0 = -\frac{3(\Gamma_E/\gamma_E)}{2\pi(a/\lambda)^2} \quad (\text{E12})$$

is the reflectance of the system on resonance with the PME mode when the split rings are symmetric ($\delta\omega = 0$), and $\lambda \equiv c/(2\pi\omega_0)$.

Equation (E6a) indicates that, when cooperative effects reduce γ_M far below $(\delta\omega)^2/\gamma_E$, a field resonant on the PMM mode does not excite the PME mode. Rather, the PMM mode is excited, and the asymmetry induced coupling between the PME and PMM modes destructively interferes with the driving of the PME mode by the incident field. The PME mode remains unexcited, and the scattered field and reflection are suppressed as indicated by Eq. (E10). A transmission resonance therefore forms when $\gamma_M \ll (\delta\omega)^2/\gamma_E$.

3. Collective mode resonance linewidths and line shifts

To determine the EM response of the array in the uniform mode approximation, one only needs in Eq. (E10) collective line shifts $\delta_{E,M}$ and linewidths $\gamma_{E,M}$ of PME and PMM modes. In the case of cooperative interactions, these depend on the number of resonators N in the system. In Fig. 4, we show numerically calculated $\delta_{E,M}$ and $\gamma_{E,M}$ as a function of N . These are evaluated by diagonalizing \mathcal{C}_{SSR} appearing in Eq. (2). Here $\delta_{E,M}$ and γ_E rapidly reach their approximate asymptotic values for array sizes around $N \simeq 1000$. Identifying the asymptotic behavior allows an efficient calculation of the collective mode parameters, the transmittance, and reflectance in the phenomenological uniform model even for large arrays.

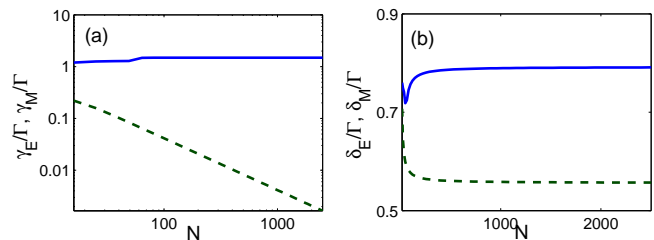


FIG. 4. The collective decay rates (a) and collective resonance frequency shifts (b) of the PME (solid blue lines) and PMM (dashed green lines) modes as functions of N the number of ASRs in a square lattice ($N_x = N_y$; $a = 0.4\lambda$; $\Gamma_E = \Gamma_M$; $u = 0.18\lambda$). The decay rate γ_E of the PME mode and the shifts δ_E and δ_M asymptotically approach constant values for sufficiently large N . The decay rate of the PMM mode $\gamma_M \propto 1/N$ for large N .

The asymptotic value of γ_E can also be determined analytically in an infinite array of SSRs ($\delta\omega = 0$) with sub-wavelength lattice spacing a . In such a system, the PME mode emits only in the forward and backward directions, corresponding to the zeroth order diffraction peak. In the absence of Ohmic losses, energy conservation therefore requires $|R|^2 + |T|^2 = 1$ in an infinite array. Therefore, according to Eqs. (E10) and (E11), an incident wave resonant on the PME mode would experience a reflectance amplitude $R_0 = -1$. At the same time Eq. (E12) relates R_0 to the collective decay rate γ_E , which then implies

$$\lim_{N \rightarrow \infty} \gamma_E = \frac{3}{2\pi(a/\lambda)^2} \Gamma_E. \quad (\text{E13})$$

This precisely corresponds to the asymptotic value of γ_E for large array sizes shown in Fig. 4.

The radiative decay rate γ_M of the PMM mode, on the other hand, asymptotically approaches zero. Since the magnetic dipoles are perpendicular to the array, they do not emit in the forward and backward directions, but as the array size increases, interference of radiation from the various meta-atoms diminishes PMM emission in other directions. The PMM mode therefore has zero emission in an infinite array. This finding is consistent with Fig. 4 which shows that asymptotically $\gamma_M \propto 1/N$, and the value of γ_M can also be extrapolated for large arrays.

Appendix F: Narrowing of the transmission resonance

In this appendix, we show how increasing the size of the metamaterial array allows one to narrow the spectral width of the transmission window and increase the group delay of a pulse passing through the array. For simplicity, we assume $\delta_M - \delta_E \ll \gamma_E$ so that we can neglect any difference between the PME and PMM resonance frequencies. We further assume that the array is sufficiently large that γ_E can be approximated by its asymptotic value [Eq. (E13)] so that $R_0 \approx -1$. In doing so,

one finds that a local maximum in transmittance occurs on PMM resonance. The reflectance amplitude on PMM resonance is thus,

$$R(\delta_M) \approx -\frac{\gamma_E \gamma_M / 4}{(\delta\omega)^2 - \gamma_E \gamma_M / 4} \quad (\text{F1})$$

When the asymmetry of ASRs satisfies $(\delta\omega)^2 \gg \gamma_E \gamma_M$, reflectance on PMM resonance is suppressed, and transmittance is enhanced.

To determine the properties of the transmission window, we assume the asymmetry is large enough so that one can express the transmittance properties to zeroth order in $\gamma_E \gamma_M / (\delta\omega)^2$. Expanding T in $\Delta - \delta_M$ one finds

$$T(\Delta) \approx 1 + \frac{i}{2} \frac{\gamma_E (\Delta - \delta_M)}{(\delta\omega)^2} - \frac{1}{4} \left(\frac{\gamma_E (\Delta - \delta_M)}{(\delta\omega)^2} \right)^2. \quad (\text{F2})$$

The width of the transmission window is determined by the intensity transmittance $|T|^2$, which can be approximated near PMM resonance using Eq. (F2). From Eq. (D2), one finds the approximate resonance width

$$w = 4\sqrt{\log 2} \frac{(\delta\omega)^2}{\gamma_E}. \quad (\text{F3})$$

The quality, or inverse spectral width, of the transmission resonance therefore varies as $1/(\delta\omega)^2$. Similarly, the

group delay is approximated by [Eq. (D3)]

$$\tau_g = \frac{\gamma_E}{2(\delta\omega)^2} \quad (\text{F4})$$

The group delay thus also scales with $1/(\delta\omega)^2$.

Since both the quality of the transmission window and the group delay of a resonant pulse scale inversely with $(\delta\omega)^2$, one could increase both quality and group delay by reducing the asymmetry. If $\delta\omega$ becomes too small, however, the intensity transmittance on PMM resonance decreases. To lowest order in $\gamma_E \gamma_M / (\delta\omega)^2$, deviation of the peak transmittance from 1, $\xi \equiv 1 - |T(\delta_M)|^2$, is

$$\xi \approx \frac{1}{2} \frac{\gamma_E \gamma_M}{(\delta\omega)^2}. \quad (\text{F5})$$

Thus, even as a smaller $\delta\omega$ enhances the resonance quality and group delay of a resonant pulse, it reduces the peak transmittance. To ensure the peak transmittance remains sufficiently high, we define a maximum tolerable deviation $\xi_{\max} \ll 1$ such that $\gamma_E \gamma_M / [2(\delta\omega)^2] < \xi_{\max}$. This imposes a lower bound on the degree to which $\delta\omega$ can be reduced while still maintaining the transmission resonance

$$(\delta\omega_{\min})^2 > \frac{\gamma_E \gamma_M}{2\xi_{\max}}. \quad (\text{F6})$$

But, as Fig. 4 illustrates, $\gamma_M \propto 1/N$, decreasing as the array gets larger. One can therefore decrease the lower bound on $(\delta\omega)^2$ by increasing N . For example, to quadruple the resonance quality and group delay while maintaining the peak transmittance, one would simultaneously quadruple the number of ASRs (doubling the side lengths of the array) and halve the asymmetry $\delta\omega$.

-
- [1] K. J. Boller, A. Imamoglu, and S. E. Harris, *Phys. Rev. Lett.* **66**, 2593 (1991).
- [2] S. E. Harris, *Physics Today* **50**, 36 (1997).
- [3] M. Fleischhauer, A. Imamoglu, and J. P. Marangos, *Rev. Mod. Phys.* **77**, 633 (2005).
- [4] L. V. Hau, S. E. Harris, Z. Dutton, and C. H. Behroozi, *Nature* **397**, 594 (1999).
- [5] C. Liu, Z. Dutton, C. H. Behroozi, and L. H. Hau, *Nature* **409**, 490 (2001).
- [6] M. D. Lukin and A. Imamoglu, *Nature* **413**, 273 (2001).
- [7] M. Fleischhauer and M. O. Scully, *Phys. Rev. A* **49**, 1973 (1994).
- [8] G. Katsoprinakis, D. Petrosyan, and I. K. Kominiis, *Phys. Rev. Lett.* **97**, 230801 (2006).
- [9] D. Budker and M. Romalis, *Nature Physics* **3**, 227 (2007).
- [10] V. I. Yudin, A. V. Taichenachev, Y. O. Dudin, V. L. Velichansky, A. S. Zibrov, and S. A. Zibrov, *Phys. Rev. A* **82**, 033807 (2010).
- [11] A. Bahrami, A. Rostami, F. Nazari, and K. Abbasian, *J. Mod. Opt.* **57**, 2021 (2010).
- [12] M. Fleischhauer and M. D. Lukin, *Phys. Rev. Lett.* **84**, 5094 (2000).
- [13] T. Chanelière, D. N. Matsukevich, S. D. Jenkins, S.-Y. Lan, T. A. B. Kennedy, and A. Kuzmich, *Nature* **438**, 833 (2005).
- [14] K. S. Choi, H. Deng, J. Laurat, and H. J. Kimble, *Nature* **452**, 67 (2008).
- [15] S. D. Jenkins, Y. O. Dudin, R. Zhao, D. N. Matsukevich, A. Kuzmich, and T. A. B. Kennedy, *J. Phys. B: At. Mol. Opt. Phys.* **45**, 124006 (2012).
- [16] S. Zhang, D. A. Genov, Y. Wang, M. Liu, and X. Zhang, *Phys. Rev. Lett.* **101**, 047401 (2008).
- [17] P. Tassin, L. Zhang, T. Koschny, E. N. Economou, and C. M. Soukoulis, *Phys. Rev. Lett.* **102**, 053901 (2009).
- [18] H. Lu, X. Liu, and D. Mao, *Phys. Rev. A* **85**, 053803 (2012).
- [19] L. Verslegers, Z. Yu, Z. Ruan, P. B. Catrysse, and S. Fan, *Phys. Rev. Lett.* **108**, 083902 (2012).
- [20] N. Papanimakis, V. A. Fedotov, N. I. Zheludev, and S. L. Prosvirnin, *Phys. Rev. Lett.* **101**, 253903 (2008).
- [21] N. Papanimakis, Y. H. Fu, V. A. Fedotov, S. L. Prosvirnin, D. P. Tsai, and N. I. Zheludev, *Appl. Phys. Lett.* **94**, 211902 (2009).
- [22] N. Liu, L. Langguth, T. Weiss, J. Kästel, M. Fleis-

- chhauer, T. Pfau, and H. Giessen, *Nat. Mater.* **8**, 758 (2009).
- [23] N. Liu, T. Weiss, M. Mesch, L. Langguth, U. Eigenthaler, M. Hirscher, C. Sonnichsen, and H. Giessen, *Nano Lett.* **10**, 1103 (2010).
- [24] L. Zhang, P. Tassin, T. Koschny, C. Kurter, S. M. Anlage, and C. M. Soukoulis, *Appl. Phys. Lett.* **97**, 241904 (2010).
- [25] J. Zhang, S. Xiao, C. Jeppesen, A. Kristensen, and N. A. Mortensen, *Opt. Express* **18**, 17187 (2010).
- [26] J. Zhang, W. Bai, L. Cai, Y. Xu, G. Song, and Q. Gan, *Appl. Phys. Lett.* **99**, 181120 (2011).
- [27] C. Kurter, P. Tassin, L. Zhang, T. Koschny, A. P. Zhuravel, A. V. Ustinov, S. M. Anlage, and C. M. Soukoulis, *Phys. Rev. Lett.* **107**, 043901 (2011).
- [28] P. Tassin, L. Zhang, R. Zhao, A. Jain, T. Koschny, and C. M. Soukoulis, *Phys. Rev. Lett.* **109**, 187401 (2012).
- [29] S. D. Jenkins and J. Ruostekoski, *Phys. Rev. B* **86**, 085116 (2012).
- [30] S. D. Jenkins and J. Ruostekoski, *New Journal of Physics* **14**, 103003 (2012).
- [31] V. A. Fedotov, N. Papasimakis, E. Plum, A. Bitzer, M. Walther, P. Kuo, D. P. Tsai, and N. I. Zheludev, *Phys. Rev. Lett.* **104**, 223901 (2010).
- [32] T. S. Kao, S. D. Jenkins, J. Ruostekoski, and N. I. Zheludev, *Phys. Rev. Lett.* **106**, 085501 (2011).
- [33] G. Adamo, J. Y. Ou, J. K. So, S. D. Jenkins, F. De Angelis, K. F. MacDonald, E. Di Fabrizio, J. Ruostekoski, and N. I. Zheludev, *Phys. Rev. Lett.* **109**, 217401 (2012).
- [34] I. M. Pryce, K. Aydin, Y. A. Kelaita, R. M. Briggs, and H. A. Atwater, *Nano Lett.* **10**, 4222 (2010).
- [35] J. Y. Ou, E. Plum, J. Zhang, and N. I. Zheludev, *Nature Nanotech.* **8**, 252 (2013).
- [36] V. A. Fedotov, M. Rose, S. L. Prosvirnin, N. Papasimakis, and N. I. Zheludev, *Phys. Rev. Lett.* **99**, 147401 (2007).
- [37] B. A. van Tiggelen, A. Lagendijk, and A. Tip, *J. Phys. Cond. Mat.* **2**, 7653 (1990).
- [38] O. Morice, Y. Castin, and J. Dalibard, *Phys. Rev. A* **51**, 3896 (1995).
- [39] J. Ruostekoski and J. Javanainen, *Phys. Rev. A* **55**, 513 (1997).
- [40] J. Ruostekoski and J. Javanainen, *Phys. Rev. A* **56**, 2056 (1997).
- [41] J. Javanainen, J. Ruostekoski, B. Vestergaard, and M. R. Francis, *Phys. Rev. A* **59**, 649 (1999).
- [42] S. D. Jenkins and J. Ruostekoski, *Phys. Rev. A* **86**, 031602(R) (2012).
- [43] M. Ricci, N. Orloff, and S. M. Anlage, *Appl. Phys. Lett.* **87**, 034102 (2005).
- [44] N. Lazarides and G. P. Tsironis, *Applied Physics Letters* **90**, 163501 (2007).
- [45] C. Du, H. Chen, and S. Li, *Journal of Physics: Condensed Matter* **20**, 345220 (2008).
- [46] J. Gu, R. Singh, Z. Tian, W. Cao, Q. Xing, M. He, J. W. Zhang, J. Han, H.-T. Chen, and W. Zhang, *Appl. Phys. Lett.* **97**, 071102 (2010).
- [47] A. L. Rakhmanov, V. A. Yampol'skii, J. A. Fan, F. Capasso, and F. Nori, *Phys. Rev. B* **81**, 075101 (2010).
- [48] V. Savinov, A. Tsiatmas, A. R. Buckingham, V. A. Fedotov, P. A. J. de Groot, and N. I. Zheludev, *Sci. Rep.* **2**, 450 (2012).
- [49] A. Zangwill, *Modern Electrodynamics* (Cambridge University Press, Cambridge, 2013).